Expression and Characterization of Four Recombinant Human Dihydrodiol Dehydrogenase Isoforms: Oxidation of *trans*-7,8-Dihydroxy-7,8-dihydrobenzo[*a*]pyrene to the Activated *o*-Quinone Metabolite Benzo[*a*]pyrene-7,8-dione[†,‡]

Michael E. Burczynski,[§] Ronald G. Harvey,[||] and Trevor M. Penning*[,§]

Department of Pharmacology, University of Pennsylvania School of Medicine, Philadelphia, Pennsylvania 19104-6084, and The Ben May Institute, University of Chicago, Chicago, Illinois 60637

Received November 3, 1997; Revised Manuscript Received March 11, 1998

ABSTRACT: The bioactivation of polycyclic aromatic hydrocarbons (PAHs) to their ultimate carcinogenic forms proceeds via the formation of proximate carcinogen *trans*-dihydrodiols. Previous studies demonstrated that rat liver 3α-hydroxysteroid dehydrogenase/dihydrodiol dehydrogenase (3α-HSD/DD), a member of the aldo−keto reductase (AKR) superfamily, oxidizes PAH *trans*-dihydrodiols to redox-cycling *o*-quinones. Multiple closely related AKRs exist in human liver; however, it is unclear which, if any, participate in PAH activation by catalyzing the $NADP^+$-dependent oxidation of PAH *trans*-dihydrodiols. In this study, cDNAs encoding four human DD isoforms were isolated from HepG2 cells using isoform-selective RT-PCR. The recombinant proteins were overexpressed in *Escherichia coli*, purified to homogeneity, and kinetically characterized. Calculation of K_M and k_{cat} values of each isoform for model substrates revealed that they possessed enzymatic activities assigned to native human liver DD1, DD2, DD4, and type 2 3α-HSD (DDX) proteins. The ability of human DDs to oxidize the potent proximate carcinogen (±)-*trans*-7,8-dihydroxy-7,8-dihydrobenzo[*a*]pyrene (BP-diol) was then examined. A reverse phase HPLC radiochemical assay demonstrated that all four isoforms oxidize (±)-BP-diol in the following rank order: DD2 > DD1 > DD4 > DDX. Each DD consumed the entire racemic BP-diol mixture, indicating that both the minor (+)-*S*,*S*- and major (−)-*R*,*R*-stereoisomers formed in vivo are substrates. First-order decay plots showed that DD1 and DD2 displayed preferences for one of the stereoisomers, and circular dichroism spectroscopy indicated that this isomer was the (+)-7*S*,8*S*-enantiomer. The products of these reactions were trapped as either glycine or thiol ether conjugates of benzo[*a*]-pyrene-7,8-dione (BPQ), indicating that the initial oxidation product was the reactive BPQ. Thus, human liver possesses multiple AKRs which contribute to PAH activation by catalyzing the $NADP^+$-dependent oxidation of PAH *trans*-dihydrodiols to redox-active *o*-quinones.

Polycyclic aromatic hydrocarbons (PAH)[1] are ubiquitous environmental pollutants and suspect human carcinogens which require metabolic activation to exert their deleterious effects (*2*). Benzo[*a*]pyrene (B[*a*]P), a representative PAH, can be activated via a stereoselective route which involves initial epoxidation by enzyme members of the cytochrome P-450s (CYP) to form an arene oxide and subsequent hydrolysis by epoxide hydrolase to yield the potent proximate carcinogen (−)-7*R*,8*R*-*trans*-dihydroxy-7,8-dihydrobenzo[*a*]-pyrene (BP-diol) (*2*, *3*). Two enzyme pathways can compete for this metabolite to further activate the proximate carcinogen (Scheme 1).

The first pathway involves members of the CYP superfamily which catalyze secondary epoxidation at the 9,10

† This work was supported by NCI Grants CA39504 and CA55711 awarded to T.M.P., ACS Grant CN-22 and NCI Grant CA67937 awarded to R.G.H., and a Pharmaceutical Research and Manufacturers of America Foundation Advanced Predoctoral Fellowship awarded to M.E.B.

‡ A preliminary account of this work was presented at the eighty-eighth annual meeting of the American Association for Cancer Research, San Diego, CA, April 13−16, 1997.

* Address for correspondence: Department of Pharmacology, University of Pennsylvania School of Medicine, 3620 Hamilton Walk, Philadelphia, PA 19104-6084. Telephone: (215) 898-9445. Fax: (215) 573-2236. E-mail: penning@pharm.med.upenn.edu.

§ University of Pennsylvania School of Medicine.

|| University of Chicago.

[1] Abbreviations: AKR, protein members of the aldo−keto reductase superfamily; androsterone, 5α-androstan-3α-ol-17-one; benzenedihydrodiol, (±)-*trans*-1,2-dihydroxy-3,5-cyclohexadiene; (±)-*anti*-BPDE, (±)-*anti*-7,8-dihydroxy-9,10-epoxy-7,8,9,10-tetrahydrobenzo[*a*]pyrene; B[*a*]P, benzo[*a*]pyrene; BP-diol, (±)-*trans*-7,8-dihydroxy-7,8-dihydrobenzo[*a*]pyrene; BPQ, benzo[*a*]pyrene-7,8-dione; CYP, protein members of the P450 superfamily; DD, dihydrodiol dehydrogenase (*trans*-1,2-dihydrobenzene-1,2-diol dehydrogenase, EC 1.3.1.20); DMSO, dimethyl sulfoxide; GSH, glutathione; GST, protein members of the glutathione *S*-transferase superfamily; 3α-HSD, 3α-hydroxysteroid dehydrogenase (EC 1.1.1.213, also AKR1C9[2]); IPTG, isopropyl β-D-thiogalactoside; PAH, polycyclic aromatic hydrocarbon(s); ROS, reactive oxygen species; RP-HPLC, reverse phase high-performance liquid chromatography; SDS−PAGE, sodium dodecyl sulfate−polyacrylamide gel electrophoresis; SQ, semiquinone anion radicals.

[2] The nomenclature for the aldo−keto reductase superfamily was recommended by Jez et al., at the 8th International Symposium on Enzymology and Molecular Biology of Carbonyl Metabolism, San Diego, CA, June 24−July 3, 1996 (*1*).

S0006-2960(97)02725-6 CCC: $15.00
Published on Web 04/22/1998

Scheme 1: Pathways Responsible for the Activation of *trans*-Dihydrodiols of PAH and the Reaction Sequence Catalyzed by Dihydrodiol Dehydrogenase(s)

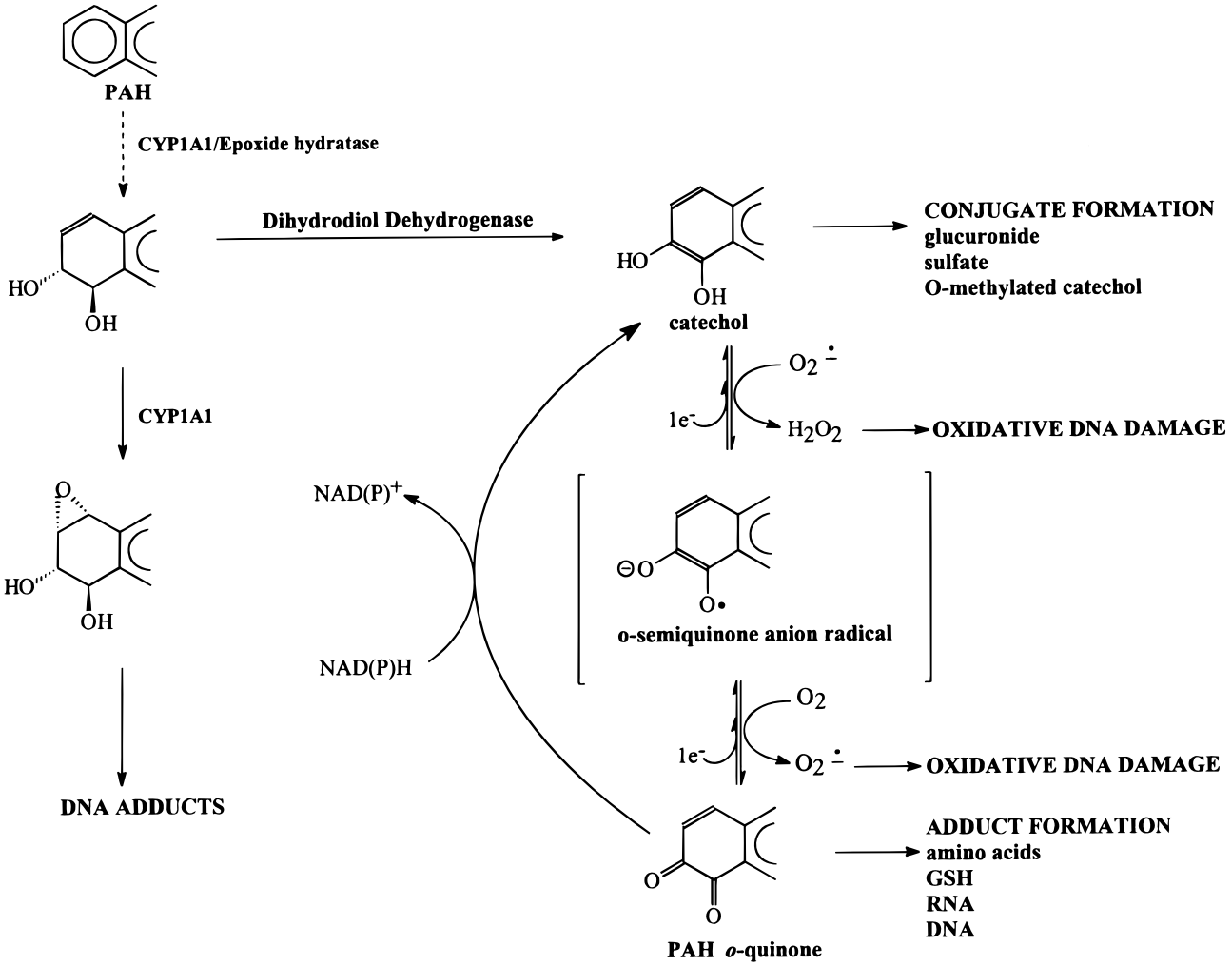

positions to yield (±)-*anti*-7,8-dihydroxy-9,10-epoxide-7,8,9,-10-tetrahydrobenzo[*a*]pyrene (*anti*-BPDE) (*3*, *4*). The second pathway involves rat liver 3α-hydroxysteroid/dihydrodiol dehydrogenase (3α-HSD/DD), a member of the aldo−keto reductase (AKR) superfamily, which can oxidize BP-diol to the corresponding *o*-quinone, benzo[*a*]pyrene-7,8-dione (BPQ) (*5*, *6*).

These pathways can represent potential detoxication routes since both the diol-epoxide and *o*-quinone metabolites of BP-diol can form water-soluble, glutathione (GSH) conjugates (*7*, *8*). Importantly, *anti*-BPDE can also form DNA adducts, is highly mutagenic and tumorigenic, and acts as an initiator in mouse skin and murine lung tumor models of carcinogenesis (*9*−*13*). Generation of BPQ may have similar deleterious consequences. BPQ has the potential to form covalent DNA adducts (stable and depurinating) and by redox cycling can generate reactive oxygen species (ROS) which can form more than 20 different types of oxidatively damaged DNA bases. One damaged base often assayed as a dosimeter of such genetic damage is 8-oxo-2-deoxyguanosine, which can lead to G to T transversions commonly observed in mutations of both proto-oncogenes and tumor supressor genes (*14*).

We have found that in isolated rat hepatocytes *anti*-BPDE and BPQ are produced to an equal extent from BP-diol (*15*). We have shown that BPQ is a reactive Michael acceptor that will form adducts with cellular nucleophiles, including GSH and DNA (*8*, *16*). Indeed, in model studies, BPQ and *anti*-BPDE formed deoxyguanosine adducts in calf thymus DNA to an equal extent (*16*). The formation of BPQ proceeds via the intermediate catechol which undergoes two one-electron oxidations to yield *o*-semiquinone (SQ) radicals and ROS on route to the *o*-quinone (*17*). By entering futile redox cycles, the *o*-quinone can generate SQ radicals and ROS multiple times. This mechanism of free radical amplification leads to extensive oxidative damage of DNA, including strand scission of phage DNA in vitro (*18*) and strand scission of genomic DNA in suspensions of rat hepatocytes (*19*). Thus, the pathway of PAH metabolism initiated by rat DD can contribute to the spectrum of genetic damage associated with PAH carcinogenesis.

Multiple enzymes exist in human liver which are capable of oxidizing benzenedihydrodiol and have been referred to as dihydrodiol dehydrogenases (DD1−DD4) (*20*). However, these enzymes have not been characterized with respect to their ability to oxidize proximate carcinogen PAH *trans*-dihydrodiols. Recently, several cDNAs encoding human dihydrodiol dehydrogenases have been isolated and in some cases expressed (*21*−*24*). They are all members of the AKR superfamily, but none of the recombinant proteins were assessed for their ability to turn over PAH metabolites. The human DD isoforms display a remarkable degree of amino

Table 1: Oligonucleotide Primers Used for Isoform-Selective RT-PCR of Four Human DD cDNAs

isoform	5′ primer[a]	3′ primer[b]
DD1	5′-CCAG**CCATG**GATTCGAAATAT-3′	3′-CCATGTTAATATTCATCAGAG-5′
DD2	5′-ACAG**CCATG**GATTCGAAATAC-3′	3′-TCCATGTTAATATTCATCAGAA-5′
DD4	5′-**CCATG**GATCCCAAATATCAGC-3′	3′-TCTATGCTAATATTCATCTGAA-5′
DDX	5′-CAGG**CCATG**GATTCCAAACAG-3′	3′-TCCATGTTAATATTCATCTGAAT-5′

[a] *Nco*I-engineered (CC)ATG start codons are bold. [b] Stop codons are underlined.

acid conservation with a sequence identity greater than 85% (and in one case, 98%). The nomenclature for associating closely related DD cDNAs with their respective enzyme activities has not been consistent throughout the primary literature. We have recently developed a systematic nomenclature for the AKR superfamily, and assignments of human DDs to the AKR1C subfamily (*1*) have been aided by the recent characterization of recombinant DDs by Hara et al. (*25*).

These studies sought first to isolate several cDNAs for human DD isoforms from a reliable source (human hepatoma cells) and to unambiguously establish the identity of the encoded recombinant proteins using functional assays. Our studies also show that four DD isoforms oxidize both the major (−)-7*R*,8*R*- and minor (+)-7*S*,8*S*-enantiomers of BP-diol formed in vivo. Oxidation of BP-diol by human DDs results in the formation of the activated *o*-quinone BPQ which is capable of redox cycling and generating oxidatively damaged DNA inside PAH-exposed cells. Thus, in addition to the CYP superfamily, human AKRs appear to form yet another important superfamily of (de)toxication enzymes involved in PAH metabolism and activation.

MATERIALS AND METHODS

Chemicals and Reagents. Cell culture media and reagents were obtained from Gibco BRL Life Technologies, Inc. (Gaithersburg, MD). Restriction enzymes were purchased from New England Biolabs (Beverly, MA). The goat anti-rabbit IgG−horseradish peroxidase conjugate and 4-chloro-1-naphthol were from Bio-Rad (Hercules, CA). Benzene-dihydrodiol was synthesized according to published procedures (*5*). β-NAD^+ and $NADP^+$ nucleotide cofactors were obtained from Boehringer Mannheim Biochemicals (Indianapolis, IN). 1-Acenaphthenol and 1-indanol were purchased from Aldrich Chemical Co. (Milwaukee, WI). Androsterone was purchased from Steraloids (Wilton, NH). Unlabeled (±)-BP-diol and BPQ were synthesized according to published procedures (*26*, *27*). [1,3-^{3}H]BP-diol (1180 mCi/mmol) and [1,3-^{3}H]BPQ (383 mCi/mmol) were purchased from the National Cancer Institute Radio-Chemical Carcinogen Reference Standard Repository at Chemsyn Science Labs (Lenexa, KS). All solvents were HPLC grade, and all other chemicals used were of the highest grade available. **Caution:** All PAHs are potentially hazardous and should be handled in accordance with NIH Guidelines for the Laboratory Use of Chemical Carcinogens.

Cell Culture. The HepG2 human hepatoma cell line was obtained from American Type Culture Collection (ATCC HB8065) and maintained in Eagle's minimal essential medium (MEM) supplemented with 10% heat-inactivated fetal bovine serum, 1% L-glutamine, 100 units of penicillin/mL, and 10 μg of streptomycin/mL. Cells were incubated at 37 °C in a humidified atmosphere containing 5% CO_2 and were passaged every 4 days at a 1:10 dilution.

Oligonucleotide Synthesis. Oligonucleotides containing unique 3′ nucleotides matching each targeted isoform of interest (Table 1) were synthesized in the Department of Genetics DNA sequencing facility at the University of Pennsylvania. *Nco*I-engineered ATG start codons (CCATG) were included in the 5′ oligonucleotides to facilitate the in-frame subcloning of PCR-amplified DD coding regions into the prokaryotic expression vector pET16b (Novagen).

Isoform Selective RT-PCR of Four Human DD cDNAs. A HepG2 first-strand cDNA library was prepared by isolating mRNA from a confluent 100 mm diameter plate of HepG2 cells (~10^7 cells) using Trizol reagent (Gibco BRL). Oligo-dT primers were added to 1 μg of a total RNA sample, and HepG2 mRNA was reverse transcribed using 200 units of Superscript II RNAse H^- Reverse Transcriptase (Gibco BRL) at 55 °C for 2 h. Aliquots (1, 2, or 5 μL) of the first-strand cDNA library were mixed with 5′ and 3′ isoform-specific primers (0.2 mM), dNTPs (0.4 mM), and 2 units of Vent DNA polymerase (NEB) in a final 1× reaction buffer volume of 50 μL. PCRs were temperature-cycled using the following conditions: 94 °C for 1 min (denaturation), 50 °C for 1 min (annealing), and 72 °C for 1.5 min (extension) for 30 cycles. Following PCR amplification, reaction mixtures were electrophoresed into a 1% agarose gel and 1 kb fragments were isolated using the Qiaquik gel extraction kit (Qiagen).

Plasmid Constructs. PCR-amplified cDNAs were ligated with T4 DNA ligase into the TA cloning vector pCRII (Invitrogen) using the Fast Link DNA ligation kit (Epicentre) to yield pCRII−DD constructs. Positive inserts were verified by dideoxy sequencing at the Department of Genetics DNA sequencing facility at the University of Pennsylvania. Coding regions of DD2, DD4, and DDX (in the SP6 orientation) were excised from pCRII using *Nco*I and *Bam*HI and were inserted into the *Nco*I−*Bam*HI sites of the prokaryotic expression vector pET16b (Novagen). Utilization of the *Nco*I site in pET16b intentionally results in the loss of the histidine tag so that expressed DDs contain only the deduced amino acid sequence. DD1 amplified from HepG2 cells contained an apparent missense mutation. As an alternative, the cDNA for wild-type DD1 was excised from a pBluescript−human colon DD construct (*28*) (generously provided by P. Ciaccio and K. Tew) and subcloned into the *Kpn*I−*Sma*I sites of the superlinker vector pSE280 (Invitrogen) which after digestion with *Sma*I and *Xho*I allowed insertion of the DD1 coding region into the filled-in *Nco*I and sticky-end *Xho*I sites of pET16b.

Prokaryotic Expression of Four Human DD Isoforms. pET16b−DD constructs were transformed into the *Escherichia coli* expression strain BL21-DE3, grown to an OD_{600} of 0.6, and then induced for 3 h with 1 mM IPTG. Bacterial sonicates were prepared and screened for the presence of DD activity by measuring the oxidation of androsterone (DD4) or 1-acenaphthenol (DD1, DD2, and DDX). SDS−

PAGE followed by Western blot analysis confirmed the presence of the appropriately sized recombinant DD protein in bacterial sonicates.

Western Blot Analysis. Portions of bacterial sonicates (15 μg) or purified proteins (1.5 μg) were boiled for 5 min and cooled on ice, and proteins were separated by SDS−PAGE and electrotransferred to nitrocellulose filters. Filters were incubated with polyclonal rabbit anti-rat 3α-HSD antiserum (*29*) at a 1:1000 dilution. Immunoblots were developed by incubation with the goat anti-rabbit IgG−horseradish peroxidase conjugate using hydrogen peroxide and 1-chloro-4-naphthol as a chromogen. No bands were observed with preimmune serum.

Purification of Four Recombinant Human DD Isoforms from E. coli. Purification of human DD isoforms was achieved from 4 L cultures of BL21-DE3 cells using the existing procedure for the purification of recombinant rat liver 3α-HSD/DD (*30*) following induction by IPTG. Throughout the purification, peak fractions were collected, assayed with androsterone (DD4) or 1-acenaphthenol (DD1, DD2, and DDX), and visualized by SDS−PAGE with Coomassie blue staining. The homogeneity of each preparation was confirmed by SDS−PAGE and Western blotting. Protein determinations were by the Bradford method (*31*). The final specific activities of DD1, DD2, DD4, and DDX for 1-acenaphthenol were 2.1, 2.5, 0.21, and 2.8 μmol min^{-1} mg^{-1}, respectively. Samples were aliquoted and stored in a final buffer consisting of 20 mM potassium phosphate (pH 7.0) containing 100 mM EDTA and 1 mM β-mercaptoethanol in 30% glycerol at −70 °C.

Spectrophotometric Assays and Kinetic Characterization of Four Human DD Isoforms. K_M and V_{max} values for substrate oxidation were obtained by varying the substrate concentration at a constant saturating cofactor concentration (2.3 mM $NADP^+$) in 1.0 mL systems containing 100 mM potassium phosphate buffer (pH 7.4). Reactions were carried out at 25 °C. Small molecule substrates (1-acenaphthenol, 1-indanol, and benzenedihydrodiol) were dissolved in methanol; the steroid substrate androsterone was dissolved in acetonitrile. The final concentration of organic solvent in the assay was 4% which did not affect enzyme activity. Initial velocities at each substrate concentration were determined on a Beckman DU640 spectrophotometer by measuring the change in absorbance of the pyridine nucleotide at 340 nm ($\epsilon = 6270$ M^{-1} cm^{-1}). Actual values of the kinetic constants were determined using ENZFITTER to fit untransformed data (substrate concentration vs initial rate) to a hyperbolic equation to provide estimates of K_M and V_{max} and their associated standard errors (*32*).

RP-HPLC Radiochemical Assay for the Oxidation of BP-Diol Catalyzed by Four Human DD Isoforms. Purified recombinant DDs (12.5 μg) were incubated in 0.1 mL assays of 50 mM glycine buffer (pH 9.0) containing 2.3 mM $NADP^+$ and 20 μM [^{3}H]BP-diol (100 000 cpm/nmol). The radiolabeled [^{3}H]BP-diol substrate was dissolved in DMSO, and the final organic solvent concentration was 8% to ensure complete solubility of BP-diol. This concentration of DMSO significantly reduces the rate of oxidation of 1-acenaphthenol by 55, 28, 57, and 43% for DD1, DD2, DD4, and DDX, respectively. Thus, the initial velocities reported for BP-diol oxidation in 8% DMSO represent corrected values. Reactions were initiated by addition of radiolabeled substrate and the mixtures incubated over a 1−3 h time course at 37 °C. At appropriate time points, reactions were quenched by injection directly onto the HPLC system. Control incubations were performed in the absence of either $NADP^+$ or recombinant enzyme.

Prior to each experiment, fresh solutions of radiolabeled [^{3}H]BP-diol were prepared and their radiochemical purity was checked by RP-HPLC. A modified RP-HPLC analysis (*33*) was conducted by injecting aliquots (50 μL) onto a Beckman System Gold RP-HPLC system using a Zorbax ODS column (25 cm × 4.6 mm; Dupont Co., Wilmington, DE) connected to a variable-wavelength UV/Vis detector (System Gold Programmable Detector Module 166) set at 254 nm. Compounds were eluted isocratically using 70:30 methanol/water (v/v) over a period of 30 min. The solvent flow rate was 1.0 mL/min, and the chromatographic system was operated at ambient temperature. PAH metabolites were identified by comparison of retention times with known standards. The amount of BP-diol remaining was quantified by counting the total counts per minute under the substrate [^{3}H]BP-diol peak at each time point and using the specific radioactivity to calculate the nanomoles of substrate present.

Stereochemical Course of trans-Dihydrodiol Oxidation. The enantiomeric selectivity of the purified dehydrogenases for the stereoisomer(s) of racemic BP-diol was determined by measuring the CD spectrum of the unreacted dihydrodiol that remained after incubation of the racemic substrate with the recombinant enzyme. Incubations were conducted in 10 mL of 50 mM glycine buffer (pH 9.0) containing 2.3 mM $NADP^+$ and 50 μM BP-diol solubilized in 8% dimethyl sulfoxide. Following addition of the purified enzyme (100 μg), the reaction mixtures were incubated at 37 °C for the appropriate time intervals (until 50% of the substrate was utilized) and then the reactions terminated by extraction of the dihydrodiols with ethyl acetate (3 × 10 mL aliquots). The organic solvent was dried with anhydrous sodium sulfate and then removed under reduced pressure. The resulting residues were chromatographed on 250 μm silica gel thin layer chromatography plates using chloroform/ethyl acetate (1:1) as the running solvent. The unreacted diols were visualized under UV irradiation and extracted from the silica with ethanol. The diols were redissolved to give solutions with an A_{367} of 1.0 absorbance unit/mL at their UV wavelength of maximum absorbance ($\lambda_{max} = 367$ nm). CD spectra were recorded on an Aviv model 60DS instrument at room temperature using a quartz cell with a 1 cm path length. CD spectra were plotted as millidegrees of ellipticity versus wavelength.

Scintillation Counting. Fractions were collected in 0.5 min intervals and counted in 5 mL of EcoLite (ICN Biomedicals, Inc., Irvine, CA) in a Tracor Analytical scintillation counter with a machine efficiency of 53% for tritum and reported as corrected counts per minute.

RESULTS

Isolation of Four Human Dihydrodiol Dehydrogenase cDNAs from a HepG2 Human Hepatoma Cell Line. Examination of the specificity of AKRs expressed in human liver for PAH *trans*-dihydrodiols requires a reliable source of human tissue or the ability to clone human DDs from a well-established liver-derived cell line. We used the latter approach and synthesized isoform-specific oligonucleotide

Table 2: Nucleotide Sequence Identities of the Four cDNAs Encoding Human DD Isoforms

PCR-amplified cDNA	100% nucleotide identity common names (GenBank IDs)[a]	98−99% nucleotide identity common names (GenBank IDs)	new AKR nomenclature[b]
DD1	none	20α(3α)-HSD, c32 (HSU05684)	AKR1C1
DD2	none	type 3 3α-HSD, c81RACE (HSU05598)	AKR1C2
DD4	chlordecone reductase (HUMCCDR)	type 1 3α-HSD, HAKRa (S68287)	AKR1C4
DDX	human open reading frame (HUMORFAA)	type 2 3α-HSD, HAKRb (S68288)	AKR1C3

[a] Comparison with open reading frames deposited in GenBank. [b] Taken from Jez et al. (*1*).

Table 3: Purification Schemes for Four Recombinant Human Dihydrodiol Dehydrogenase Isoforms[a]

protein	purification step	volume (mL)	total protein (mg)	total activity (μmol/min)	specific activity (μmol min^{-1} mg^{-1})	purification factor (-fold)	yield (%)
	sonicate	61	460	59	0.13		
DD1	DE52 cellulose	16	23	46	2.0	15	78
	Blue Sepharose	8	20	42	2.1	16	71
	sonicate	77	510	42	0.08		
DD2	DE52 cellulose	18	19	39	2.1	25	93
	Blue Sepharose	11	15	37	2.5	31	88
	sonicate	44	270	4.6	0.02		
DD4	DE52 cellulose	12	23	2.8	0.12	6	61
	Blue Sepharose	8	13	2.7	0.21	11	59
	sonicate	51	310	65	0.21		
DDX	DE52 cellulose	56	25	51	2.0	10	78
	Blue Sepharose	5	12	34	2.8	13	52

[a] Specific activities throughout the purifications were measured using 75 μM androsterone (DD4) or 1 mM 1-acenaphthenol (DD1, DD2, and DDX) as the substrate in reaction mixtures containing 100 mM KPO_4 (pH 7.0) and 2.3 mM NAD^+ at 25.0 °C.

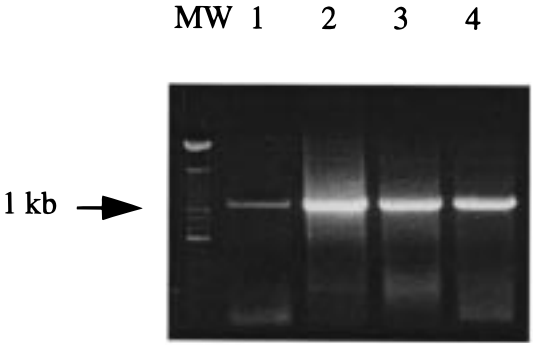

FIGURE 1: Isoform-selective RT-PCR of four human dihydrodiol dehydrogenases. RT-PCR amplifications from a HepG2 first-strand cDNA library were performed as described, and aliquots (10 μL) of each reaction mixture were electrophoresed on a 1% agarose gel stained with ethidium bromide to visualize DNA bands: lane 1, DD4; lane 2, DDX; lane 3, DD1; and lane 4, DD2.

primers matching sequences for previously cloned human DDs. Isoform-selective PCR was then performed to isolate cDNAs from a human hepatoma cell line (HepG2) first-strand cDNA library. Distinct clones spanning the coding regions of four dihydrodiol dehydrogenases were PCR-amplified (Figure 1) and sequenced. DD3 (aldehyde reductase) was not isolated in these studies since its sequence identity with rat 3α-HSD is low (40%) compared to those of the other four DDs (>70%). Comparison with previously deposited GenBank nucleotide sequences revealed the identities of the four clones as DD1, DD2, DD4, and a clone given the name DDX (Table 2).

Prokaryotic Expression and Purification of Four Recombinant Human Dihydrodiol Dehydrogenases. To obtain recombinant human DD isoforms for subsequent enzymatic studies, the four distinct cDNAs were subcloned into the prokaryotic expression vector pET16b and overexpressed in the *E. coli* expression strain BL21-DE3. Each of the four DD proteins was purified to homogeneity as described in Materials and Methods, and purification schemes for each of the DDs are presented (Table 3). Each protein was obtained in milligram amounts. The degree of purification was between 13- and 30-fold, and the overall yields were high. The purity of each DD isoform was established by SDS−PAGE followed by Coomassie staining and Western blot analysis (Figure 2). Western blot analysis detected single immunopositive bands of ∼37 kDa for all four isoforms, consistent with previous reports (*20*).

Kinetic Characterization of Recombinant DDs and Their Identity with Native DDs Previously Isolated from Human Liver. The extraordinary conservation of amino acid residues among certain members of the AKR superfamily dictated the unambiguous identification of the recombinant DD isoforms cloned in these studies. For example, the amino acid sequences deduced from the four cDNAs isolated differ in amino acid identity by as little as 2% (DD1 vs DD2) up to only 17% (DD1 vs DD4). The functional identity of the recombinant enzymes was established by measuring their catalytic activities using several common substrates. K_M and k_{cat} values obtained for the recombinant proteins were compared with values previously reported (*20*, *34*) for native DD isoform activities (Table 4). Comparison of K_M and k_{cat} values revealed very good agreement between values for the recombinant enzymes and those previously reported for native enzymes. Discrimination between the closely related DD1 and DD2 isoforms was achieved on the basis of three kinetic characteristics: (1) rDD2 possessed a measurable rate of androsterone oxidation (3α-HSD activity) while DD1 did not; (2) rDD2 had a much higher K_M for 1-indanol than rDD1; and (3) rDD2 had an extremely high K_M (millimolar range) for benzenedihydrodiol. This comparison shows that the cDNAs we initially designated DD1, DD2, and DD4 were correctly assigned. DDX does not possess kinetic properties

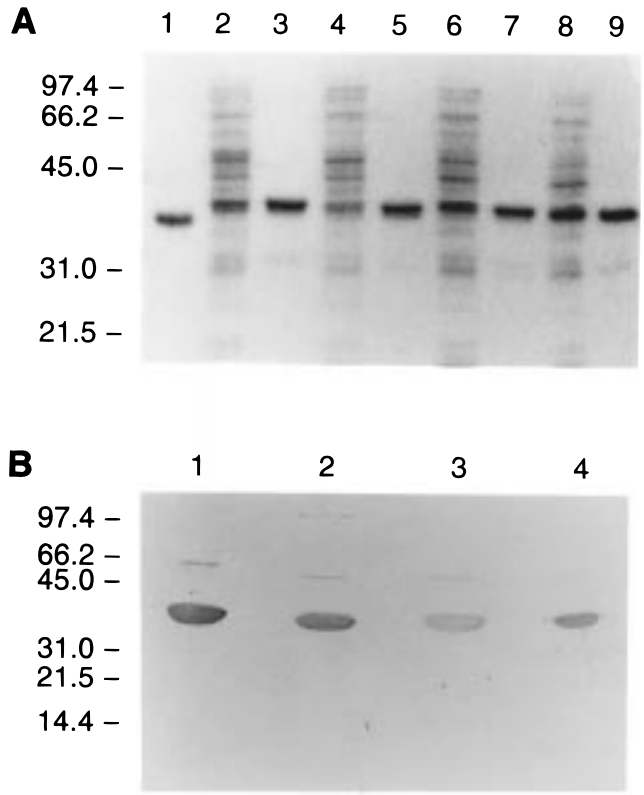

FIGURE 2: SDS−PAGE and Western blot analysis of purified human DD isoforms. (A) Purification of DD isoforms from *E. coli* lysates. Fifteen micrograms of each lysate (even-numbered lanes) and 1.5 μg of each purified protein (odd-numbered lanes) were loaded and visualized with Coomasie Blue R-250: lane 1, recombinant rat 3α-HSD; lanes 2 and 3, DD1; lanes 4 and 5, DD2; lanes 6 and 7, DD4; and lanes 8 and 9, DDX. (B) Immunoblot analysis of recombinant DD isoforms. One microgram of each purified protein was loaded per lane. Proteins were detected using a 1:1000 dilution of polyclonal rabbit anti-rat 3α-HSD sera 71535 and visualized with the goat anti-rabbt IgG−horseradish peroxidase conjugate (*29*): lane 1, DD1; lane 2, DD2; lane 3, DD4; and lane 4, DDX. Positions of molecular weight standards are indicated.

Table 4: Substrate Specificity for Recombinant (and Native) Human Dihydrodiol Dehydrogenases[a]

isoform	substrate	K_M (μM)[b]	k_{cat} (min^{-1})	k_{cat}/K_M ($min^{-1}\,mM^{-1}$)
DD1	1-acenaphthenol	22 (26)	29.4	1300
	1-indanol	48 (38)	12.5 (10)	260 (263)
	androsterone	–	–	–
	benzenedihydrodiol	150 (580)	2.9 (3.2)	19 (6)
DD2	1-acenaphthenol	22 (56)	35.1	1600
	1-indanol	940 (520)	9.8 (9.5)	11 (18)
	androsterone	3.5 (8)	0.4 (0.7)	110 (88)
	benzenedihydrodiol	1800 (5000)	1.1 (1.9)	0.6 (0.4)
DD4	1-acenaphthenol	140 (500)	7.5	15
	1-indanol	170 (260)	9.5 (19)	56 (73)
	androsterone	3.5 (0.9)	1.1 (5.4)	310 (6000)
	benzenedihydrodiol	17 (24)	2.0 (2.2)	120 (92)
DDX	1-acenaphthenol	70	25	360
	1-indanol	1400	5.2	3.7
	androsterone	–	–	–
	benzenedihydrodiol	320	0.9	2.8

[a] All enzymatic reactions were performed in 100 mM KPO_4 (pH 7.4) and 2.3 mM $NADP^+$ at 25 °C. [b] Native values (in parentheses) are taken from Hara et al. (*20*) and Deyashiki et al. (*34*).

similar to those of previously purified native proteins and thus represents a novel DD isoform. It is closest in sequence

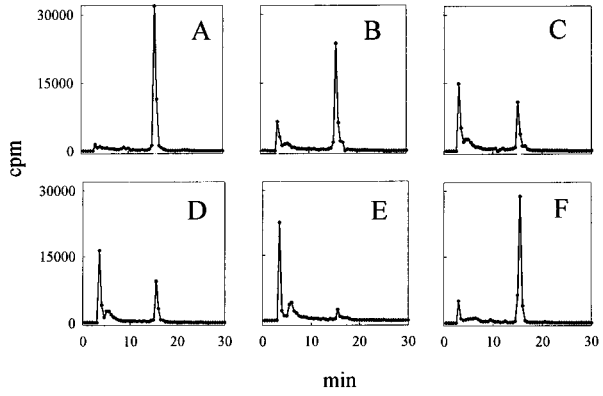

FIGURE 3: RP-HPLC assay of (±)-[1,3-^{3}H]BP-diol oxidation catalyzed by homogeneous human DD2. (±)-[1,3-^{3}H]BP-diol (20 μM, 100 000 cpm/nmol) was incubated with human DDs (12.5 μg) in 50 mM glycine buffer (pH 9.0) at 37 °C in the presence and absence of $NADP^+$ (2.3 mM), and samples were analyzed by RP-HPLC as described in Materials and Methods: panels A−E, radiochromatograms of the complete system obtained over time (0, 5, 10, 30, and 90 min, respectively) for the DD2-catalyzed oxidation of [^{3}H]BP-diol (20 μM); and panel F, radiochromatogram of the minus $NADP^+$ control after 120 min at 37 °C.

to type 2 3α-HSD, but unlike this enzyme, it does not catalyze the oxidation of androsterone (*35*).

Initial Velocities of BP-Diol Oxidation Catalyzed by Human DD Isoforms. To determine whether any of the human DD isoforms play roles in PAH carcinogen metabolism and activation, the ability of human DDs to oxidize the important proximate carcinogen (±)-[^{3}H]BP-diol was assessed. UV spectrophotometric-based assays were initially performed to determine whether BP-diol turnover by human DDs occurred. Visual inspection of cuvettes containing complete enzymatic systems for each of the four rDDs revealed a color change from clear (BP-diol) to dark purple (BPQ or its conjugates) after incubation for 1 h. For precise estimation of specific activities, a slightly modified version of a radiochemical RP-HPLC assay (*33*) was used to monitor the disappearance of the (±)-[^{3}H]BP-diol substrate (100 000 cpm/nmol) in the presence of human DDs and $NADP^+$ cofactor.

Radiochromatograms obtained over time for the DD2-catalyzed oxidation of (±)-[^{3}H]BP-diol are shown in Figure 3. There was no significant nonenzymatic rate as shown by the lack of substrate disappearance in both the minus $NADP^+$ (Figure 3F) and minus enzyme controls (data not shown). The total counts per minute in the (±)-[^{3}H]BP-diol peak remaining at each time point was used to calculate the nanomoles of BP-diol oxidized which was then plotted versus time (Figure 4). Initial velocities (Figure 4 inset) were determined for each of the four DD isoforms. The rank order of specific activities for the oxidation of (±)-BP-diol was as follows: DD2 > DD1 > DD4 > DDX. The complete disappearance of the racemic (±)-[^{3}H]BP-diol catalyzed by all four human DD isoforms indicates that these enzymes oxidize both the major (−)-7*R*,8*R*- and the minor (+)-7*S*,8*S*-stereoisomers of BP-diol formed in vivo.

Pseudo-First-Order Analysis of BP-Diol Oxidation Data. End-point determinations of the amount of BP-diol oxidized were conducted at substrate concentrations well below K_M; thus, these reactions can be regarded as simple first-order processes, and semilog plots of the fraction of substrate

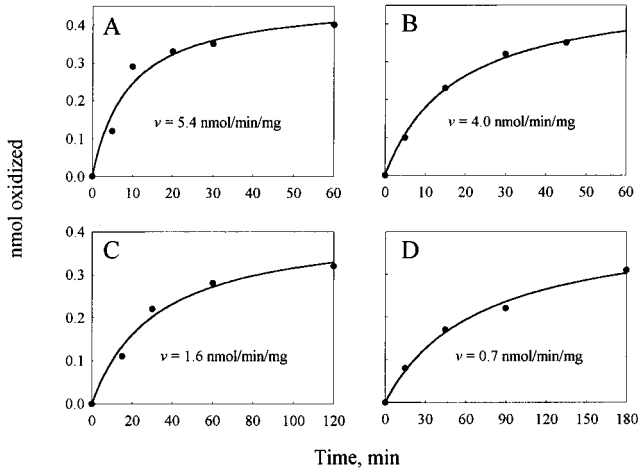

FIGURE 4: Initial progress curves for the oxidation of the proximate carcinogen (±)-[1,3-^{3}H]BP-diol catalyzed by four human DDs. Following RP-HPLC analysis, the total counts per minute in the (±)-[^{3}H]BP-diol peak remaining at each time point was used to calculate the nanomoles of BP-diol oxidized and plotted versus time. The initial velocities (insets) were calculated from the linear portion of the data as shown: (A) DD2, (B) DD1, (C) DD4, and (D) DDX.

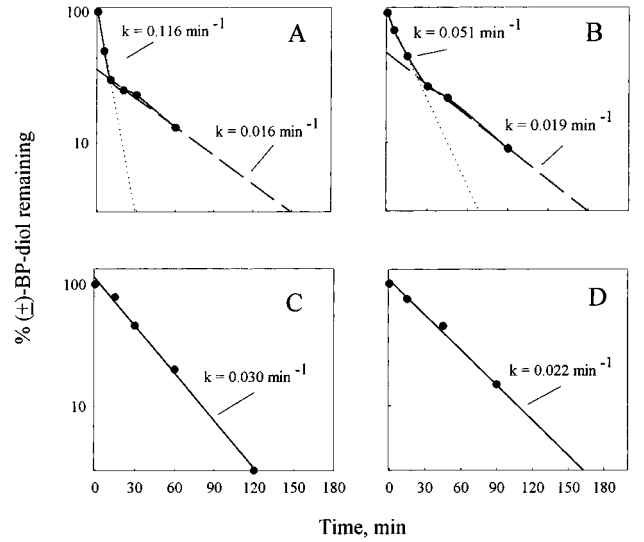

FIGURE 5: Pseudo-first-order analysis of human DD-catalyzed oxidation of the racemic (±)-[1,3-^{3}H]BP-diol. The percentage of *trans*-dihydrodiol substrate remaining (log scale) at each time point was calculated from RP-HPLC assays and plotted versus time. Estimates of the fast and slow components for DD1- and DD2-catalyzed oxidation of BP-diol were obtained by fitting a regression line to the slow component of the reaction; this line was extrapolated to the origin, and the residuals were calculated: (A) DD2, (B) DD1, (C) DD4, and (D) DDX.

remaining versus time should be linear. The data for the oxidation of BP-diol catalyzed by all four human DD isoforms were reanalyzed in this manner (Figure 5). While transformation of the data yielded the expected linear plots ($r^2 \geq 0.998$) for DDX (which possessed the slowest rate) and DD4, transformation of the data yielded increasingly curvilinear semilog plots for DD1 and DD2, indicative of a higher-order reaction consisting of both fast and slow components. Thus, although all four DD isoforms oxidize both stereoisomers of (±)-BP-diol, in some cases, one stereoisomer is oxidized more rapidly than the other.

Identification of the Preferred Stereoisomer of BP-Diol Oxidation Catalyzed by Human DDs. To identify the stereoisomer(s) of BP-diol preferentially oxidized by DD1

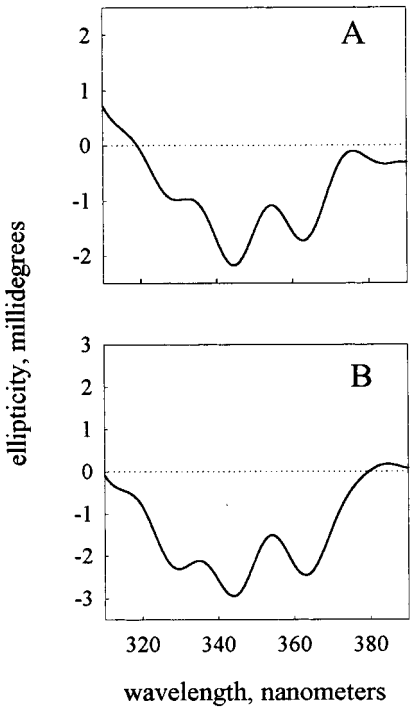

FIGURE 6: Identification of the *trans*-dihydrodiol stereoisomers preferentially oxidized by DD1 and DD2. Large-scale enzymatic oxidation reactions with BP-diol were conducted as described in Materials and Methods, and aliquots were monitored by RP-HPLC to determine the point at which 50% of the substrate had been utilized. Reaction mixtures were then extracted with ethyl acetate; unoxidized dihydrodiol substrates were isolated by thin layer chromatography, and their CD spectra were recorded. The CD spectrum of the racemic (±)-BP-diol was subtracted from the spectrum of the enantiomerically enriched substrates to determine the sign of the Cotton effect. (A) CD spectra of unreacted dihydrodiol recovered from the DD2-catalyzed reaction and (B) CD spectra of unreacted dihydrodiol recovered from the DD1-catalyzed reaction.

and DD2, large-scale incubations were conducted with racemic (±)-BP-diol and each of the purified enzymes. Incubation of DD1 or DD2 with the racemic *trans*-dihydrodiol until the rapid phase of each reaction was complete allowed CD analysis of the unreacted stereoisomer to be performed. The stereoselectivity of each enzyme for BP-diol is shown in Figure 6. The presence of a (−) Cotton effect remaining in both reactions indicates that the (+)-enantiomer was preferentially oxidized by both DD1 and DD2.

Formation of Glycine and Thiol Ether Conjugates of BPQ during the DD-Catalyzed Oxidation of BP-Diol. Rat liver 3α-HSD/DD has been shown to oxidize BP-diol to the reactive BPQ which can undergo conjugation reactions in buffer to form buffer adducts (*6*). In this study, RP-HPLC assays showed that the disappearance of BP-diol was accompanied by the appearance of two highly polar radioactive peaks (retention times of 3.5 and 5.5 min) migrating just ahead of the solvent front. To determine whether the products of BP-diol oxidation catalyzed by human DDs represent the anticipated BPQ−glycine adducts, a [^{3}H]BPQ standard was analyzed by HPLC after incubation in 70:30 methanol/H_2O (v/v) or after incubation for 60 min in the reaction buffer (50 mM glycine at pH 9.0). While the relatively nonpolar [^{3}H]BPQ normally migrates at ∼20 min under these conditions (Figure 7B), [^{3}H]BPQ incubated in

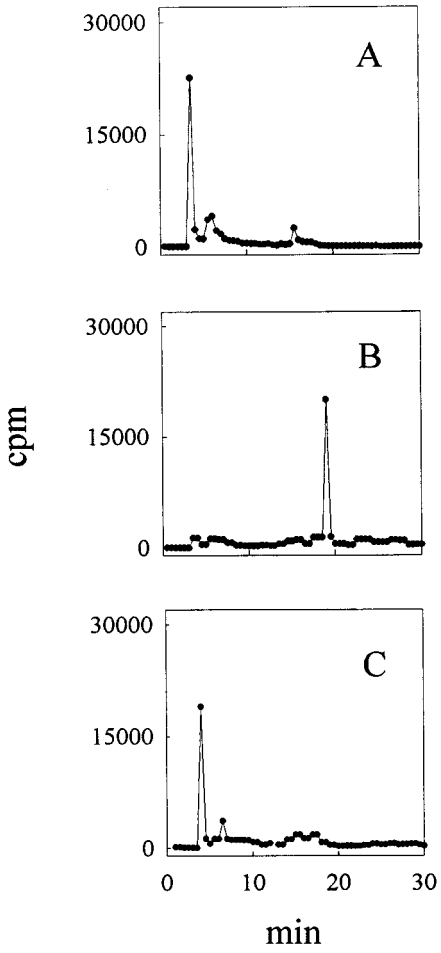

FIGURE 7: Formation of BPQ−glycine conjugates during the DD-catalyzed oxidation of BP-diol. (A) Product profile following the DD2-catalyzed oxidation of 20 μM [1,3-^{3}H]BP-diol in 50 mM glycine buffer at pH 9.0 after 90 min. (B) Radiochromatogram of 20 μM [1,3-^{3}H]BPQ. (C) Radiochromatogram of 20 μM [1,3-^{3}H]-BPQ following incubation in 50 mM glycine buffer at pH 9.0 for 90 min.

50 mM glycine readily forms two highly polar glycine conjugates (Figure 7C) which comigrate (retention times of 3.5 and 5.5 min) with products resulting from the DD-catalyzed oxidation of BP-diol (Figure 7A). This result indicates that, while DD-catalyzed oxidation of BP-diol results in production of BPQ, the electrophilic *o*-quinone readily undergoes nucleophilic attack in the presence of 50 mM glycine to yield highly polar BPQ−glycine conjugates. In additional studies, we have performed the reactions in phosphate buffer at pH 7.0 and successfully trapped the enzymatically formed BPQ as the thiol ether conjugate of 2-mercaptoethanol. This conjugate comigrates with the synthetically prepared thiol ether conjugate of BPQ which has been fully characterized (*6*). The thiol ether conjugate of BPQ is formed exclusively in the complete reaction systems containing enzyme, $NADP^+$, and BP-diol.

DISCUSSION

These studies demonstrate that four distinct DD isoforms expressed in human liver can be cloned from a human hepatoma cell line and that they play roles in PAH metabolism and activation. All four DDs catalyze the $NADP^+$-dependent oxidation of the PAH *trans*-dihydrodiol proximate carcinogen BP-diol to yield the corresponding reactive *o*-quinone BPQ. Each isoform is a member of the AKR superfamily, indicating that this family can play an important role in PAH metabolism and activation.

Our PCR results, while not rigorously quantitative, suggest that the various DD isoforms are expressed at different levels in HepG2 cells. Thus, the HepG2 cell line represents an attractive system in which to further characterize human DD activities, their role in PAH metabolism, and the regulation of their expression by xenobiotics.

BLAST search analysis of the four DD cDNAs indicated that they were 99−100% identical to previously deposited GenBank open reading frames. We designated three of the cDNAs amplified in these studies as DD1, DD2, and DD4. These assignments were validated by expressing the encoded recombinant proteins and kinetically characterizing the expressed activities. It was found that three of the four recombinant proteins had properties identical to those of the native enzymatic activities DD1, DD2, and DD4. These studies also represent the first report of the purification and enzymatic characterization of the recombinant human DD2 isoform. DD1 and DD2 differ by a single amino acid substitution at the active site (L54V), and the differences in the kinetic properties of recombinant DD1 and DD2 described here support the finding that a point mutation at this position is sufficient to convert DD1 to a DD2-like enzyme (*36*). A fourth DD isoform, DDX, did not possess kinetic characteristics consistent with any previously characterized native DD from human liver. It shares its highest sequence identity with type 2 3α-HSD (*35*), but unlike this enzyme, it does not catalyze the oxidation of androsterone when measured spectrophotometrically. Purified DDX showed no activity for androsterone oxidation in a spectrophotometric assay, whereas others reported that unpurified bacterial sonicates expressing type 2 3α-HSD possessed measurable androsterone oxidation activity (*35*). The deduced amino acid sequence for DDX differs from that reported for type 2 3α-HSD at only two residues which, on the basis of the crystal structure (*37*) of the rat liver 3α-HSD ternary complex ($E{\cdot}NADPH^+{\cdot}$testosterone), are predicted to reside on the exterior of the enzyme and should play no role in catalytic activity or substrate specificity. DDX does not represent a cloning artifact since (1) its nucleotide sequence is 100% identical to an open reading frame of a complete cDNA cloned from a human myeloblast cDNA library which was previously deposited into GenBank (accession ID HUMORFAA) and (2) DDX matches the deduced amino acid sequence for human prostatic 3α(17β)-HSD (*38*). We have argued that human prostatic 3α(17β)-HSD (and thus DDX) is essentially identical to type 2 3α-HSD and that its specific activity for androsterone oxidation in bacterial sonicates was previously reported in error (*35*).

The substrate specificity of each human DD isoform for *trans*-dihydrodiol proximate carcinogens was investigated using (±)-BP-diol. It was found that the rank order of specific activities toward 20 μM (±)-BP-diol was as follows: DD2 > DD1 > DD4 > DDX. It appears that, as is the case for many xenobiotic-metabolizing enzymes, the human DD isoforms have evolved to metabolize a diverse array of dissimilar substrates. They turn over hydroxysteroids (*20*, *34*), hydroxyprostaglandins (*25*), bile acids (*21*), narcotic analgesics (*39*), organochlorine pesticides (*40*), and now, in these studies, carcinogenic PAH *trans*-dihydrodiols.

Thus, the AKRs like the CYPs represent a major family of drug- and xenobiotic-metabolizing enzymes which are also involved in PAH activation.

Pseudo-first-order analysis of the initial progress curves demonstrated the existence of a trend toward increasing stereochemical preference as apparent specific activities for the four isoforms increased for (±)-BP-diol. Thus, DDX (lowest specific activity) and DD4 display no significant stereochemical preference, whereas DD1 and DD2 (highest specific activity) possess a distinct stereochemical preference for one of the stereoisomers. The preference for the "fast" reaction (i.e. preferential oxidation of one of the two stereoisomers) is the basis for the increasing higher specific activity of the DD isoforms toward racemic BP-diol.

Circular dichroism studies revealed that DD1 and DD2 display a 3- and 7-fold stereochemical preference, respectively, for the (+)-*S*,*S*-isomer. By contrast, pseudo-first-order rate constants for the oxidation of the (−)-7*R*,8*R*-enantiomer reveal that that there is only a 2-fold variation in the ability of the human DD isoforms to oxidize the (−)-7*R*,8*R*-isomer. Although the (−)-7*R*,8*R*-isomer is often referred to as the predominant metabolite formed in vivo in the liver, the (+)-*S*,*S*-isomer is formed to a greater extent in human lung (21%) than in liver (9%) and is also tumorigenic in murine tumor model systems (*41*). Regardless of the enantiomeric preferences demonstrated by the DD1 and DD2 isoforms, it is important to emphasize that all four DDs ultimately oxidize both the major and minor BP-diol stereoisomers formed in vivo.

BPQ, a nonpolar metabolite, was shown to be the product of human DD-catalyzed oxidation of BP-diol, and this was consistent with previous studies on rat liver 3α-HSD/DD (*6*). BPQ is a highly reactive Michael acceptor and has been previously shown to form adducts with multiple nucleophiles, including glycine and thiols (*6*). In these studies, BP-diol was first enzymatically oxidized by DD to BPQ which was then rapidly "trapped" nonenzymatically as either glycine or thiol−ether conjugates.

The ability of human DD isoforms to oxidize both isomers of the racemic BP-diol to BPQ may have important toxicological consequences. In rat (H4IIE) and human (HepG2) hepatoma cells, exposure to BPQ reduces cell viability by depleting GSH (*42*). BPQ is also a genotoxin. Disposition studies of toxicologic concentrations of BPQ exogenously applied to rat hepatocyte suspensions indicate that ∼30% of the radioactive metabolite is incorporated into cellular macromolecules (DNA, RNA, and protein) and that a significant amount is sequestered in DNA (*19*). Although covalent modification of DNA by BPQ was demonstrated, no stable deoxyguanosine−BPQ adducts were recovered, suggesting that bulky adducts were unstable and may be depurinating. Interestingly, estrogen quinones (which are structurally related to BPQ) also form depurinating adducts (*43*). Furthermore, incubation of BPQ with hepatocytes leads to extensive strand scission of genomic DNA, and in model studies with ϕX174 phage DNA, BPQ was found to be 200 times more potent as a chemical nuclease than *anti*-BPDE (*19*). Strand scission of DNA can lead to illegitimate recombination events (*44*) which could play a role in PAH carcinogenesis. PAH *o*-quinones are only mildly mutagenic in bacterial assays when compared to their corresponding diol-epoxides (*19*, *42*) but produce significant amounts of reactive oxygen species (ROS) which oxidatively damage bases in DNA. 8′-Oxo-2′-deoxyguanosine can give rise to G to T transversions (*14*) which is one of the most common mutations observed in select codons in the *H-ras* proto-oncogene and the *p53* tumor supressor gene (*45*−*48*). The production of ROS has also been linked to tumor promotion (*49*) and recently established as a component of the mitogenic stimulus evoked by oncogenic ras (*50*). Thus, production of the electrophilic Michael acceptor and redox-active metabolite BPQ may play a substantial role in the ability of PAH to act as complete carcinogens.

In summary, the studies described indicate an important role for human DDs, members of the AKR superfamily, in the metabolism and activation of PAH proximate carcinogen *trans*-dihydrodiols. They suggest that human AKRs, like the CYPs and GSTs, are part of the cellular defense utilized against xenobiotic exposure. They also raise the possibility that, like the CYPs and GSTs, human AKRs have evolved to handle toxicologic insults but in so doing may also activate certain xenobiotics. In particular, the DD isoforms oxidize the major (−)-7*R*,8*R*-stereoisomer of BP-diol formed in vivo to the activated *o*-quinone BPQ, suggesting that this alternative pathway of PAH activation can occur in humans.

REFERENCES

1. Jez, J. M., Flynn, G. F., and Penning, T. M. (1997) *Biochem. Pharmacol. 54*, 639−647.
2. Conney, A. H. (1982) *Cancer Res. 42*, 4875−4917.
3. Yang, S. K., McCourt, D. W., Roller, P. P., and Gelboin, H. V. (1976) *Proc. Natl. Acad. Sci. U.S.A. 73*, 2594−2598.
4. Yang, S. K., Mushtaq, M., and Chiu, P. L. (1985) in *Polycyclic Hydrocarbons and Carcinogenesis* (Harvey, R. G., Ed.) pp 19−34, ACS Symposium Series 283, American Chemical Society, Washington, DC.
5. Smithgall, T. E., Harvey, R. G., and Penning, T. M. (1986) *J. Biol. Chem. 261*, 6184−6191.
6. Smithgall, T. E., Harvey, R. G., and Penning, T. M. (1988) *J. Biol. Chem. 263*, 1814−1820.
7. Hesse, S., Jernstrom, B., Martinez, M., Christodoulides, L., and Ketterer, B. (1982) *Carcinogenesis 3*, 757−761.
8. Murty, V. S., and Penning, T. M. (1992) *Bioconjugate Chem. 3*, 218−224.
9. Newbold, R. F., and Brookes, P. (1976) *Nature 261*, 52−54.
10. Jeffrey, A. M., Jennette, K. W., Blobstein, S. H., Weinstein, I. B., Beland, F. A., Harvey, R. G., Kasai, H., Miura, I., and Nakanishi, K. (1976) *J. Am. Chem. Soc. 98*, 5714−5715.
11. Malaveille, C., Kuroki, T., Sims, P., Grover, P. L., and Bartsch, H. (1977) *Mutat. Res. 44*, 313−326.
12. Kapitulnik, J., Wislocki, P. G., Levin, W., Yagi, H., Jerina, D. M., and Conney, A. H. (1978) *Cancer Res. 38*, 354−358.
13. Slaga, T. J., Braken, W. J., Gleason, G., Levin, W., Yagi, H., Jerina, D. M., and Conney, A. H. (1979) *Cancer Res. 39*, 67−71.
14. Grollman, A. P., and Moriya, M. (1993) *Trends Genet. 9*, 246−249.
15. Flowers-Geary, L., Harvey, R. G., and Penning, T. M. (1995) *Carcinogenesis 16*, 2707−2715.
16. Shou, M., Harvey, R. G., and Penning, T. M. (1993) *Carcinogenesis 14*, 475−482.
17. Penning, T. M., Ohnishi, S. T., Ohnishi, T., and Harvey, R. G. (1996) *Chem. Res. Toxicol. 9*, 84−92.
18. Flowers, L., Ohnishi, S. T., and Penning, T. M. (1997) *Biochemistry 36*, 8640−8648.
19. Flowers, L., Bleczinski, W. F., Burczynski, M. E., Harvey, R. G., and Penning, T. M. (1996) *Biochemistry 35*, 13664−13672.
20. Hara, A., Taniguchi, H., Nakayama, T., and Sawada, H. (1990) *J. Biochem. 108*, 250−254.

21. Stolz, A., Hammond, L., Lou, H., Takikawa, H., Ronk, M., and Shively, J. E. (1993) *J. Biol. Chem. 268*, 10448−10457.
22. Qin, K.-N., New, M. I., and Cheng, K.-C. (1993) *J. Steroid Biochem. Mol. Biol. 46*, 673−679.
23. Ciaccio, P. J., and Tew, K. D. (1994) *Biochim. Biophys. Acta 1186*, 129−132.
24. Deyashiki, Y., Ogasawara, A., Nakayama, T., Nakanishi, M., Miyabe, Y., Sato, K., and Hara, A. (1994) *Biochem. J. 299*, 545−552.
25. Hara, A., Matsurra, K., Tamada, Y., Sato, K., Miyabe, Y., Deyashiki, Y., and Ishida, T. (1996) *Biochem. J. 31*, 373−376.
26. Fu, P. P., and Harvey, R. G. (1977) *Tetrahedron Lett.*, 2059−2062.
27. Sukumaran, K. B., and Harvey, R. G. (1980) *J. Org. Chem. 45*, 4407−4413.
28. Ciaccio, P. J., Jaiswal, A. K., and Tew, K. D. (1994) *J. Biol. Chem. 269*, 15558−15562.
29. Smithgall, T. E., and Penning, T. M. (1988) *Biochem. J. 254*, 715−721.
30. Jez, J. M., Schlegel, B. P., and Penning, T. M. (1996) *J. Biol. Chem. 271*, 30190−30196.
31. Bradford, M. M. (1976) *Anal. Biochem. 72*, 248−254.
32. Leatherbarrow, R. J. (1987) *ENZFITTER: A Non-Linear Regression Data Analysis Program for the IBM PC (and true compatibles)*, Biosoft, Cambridge, U.K.
33. Flowers-Geary, L., Harvey, R. G., and Penning, T. M. (1992) *Chem. Res. Toxicol. 5*, 576−583.
34. Deyashiki, Y., Taniguchi, H., Amano, T., Nakayama, T., Hara, A., and Sawada, H. (1992) *Biochem. J. 282*, 741−746.
35. Khanna, M., Qin, K.-N., Wang, R. W., and Cheng, K.-C. (1995) *J. Biol. Chem. 270*, 20162−20168.
36. Matsuura, K., Deyashiki, Y., Sato, K., Ishida, N., Miwa, G., and Hara, A. (1997) *Biochem. J. 323*, 61−64.
37. Bennett, M. J., Albert, R. H., Jez, J. M., Ma, H., Penning, T. M., and Lewis, M. (1997) *Structure 5*, 799−812.
38. Lin, H. K., Jez, J. M., Schlegel, B. P., Peehl, D. M., Pachter, J. A., and Penning, T. M. (1997) *Mol. Endocrinol. 11*, 1971−1984.
39. Ohara, H., Miyabe, Y., Deyashiki, Y., Matsuura, K., and Hara, A. (1995) *Biochem. Pharmacol. 50*, 221−227.
40. Molowa, D. T., Shayne, A. G., and Guzelian, P. S. (1986) *J. Biol. Chem. 261*, 12624−12627.
41. Levin, W., Buening, M. K., Wood, A. W., Chang, R. L., Kedzierski, B., Thakker, D. R., Boyd, D. R., Gadaginamath, G. S., Armstrong, R. N., Yagi, H., Karle, J. M., Slaga, T. J., Jerina, D. M., and Conney, A. H. (1980) *J. Biol. Chem. 255*, 9067−9074.
42. Flowers-Geary, L., Bleczinski, W., Harvey, R. G., and Penning, T. M. (1996) *Chem.−Biol. Interactions 99*, 55−72.
43. Stack, D. E., Byun, J., Gross, M. L., Rogan, E. G., and Cavalieri, E. L. (1996) *Chem. Res. Toxicol. 9*, 851−859.
44. Emerit, I., Keck, M., Levy, A., Feingold, J., and Michelson, A. M. (1982) *Mutat. Res. 103*, 165−172.
45. Denissenko, M. F., Pao, A., Tang, M., and Pfeifer, G. P. (1996) *Science 274*, 430−432.
46. Colapietro, A. M., Goodell, A. L., and Smart, R. C. (1993) *Carcinogenesis 14*, 2289−2295.
47. Mass, M. J., Jeffers, A. J., Ross, J. A., Nelson, G., Galati, A. J., Stoner, G. D., and Nesnow, S. (1993) *Mol. Carcinog. 8*, 186−192.
48. Puisieux, A., Lim, S., Groopman, J., and Ozturk, M. (1991) *Cancer Res. 51*, 6185−6189.
49. Ames, B. N., and Gold, L. S. (1990) *Science 227*, 375−381.
50. Irani, K., Xia, Y., Zweier, J. L., Sollott, S. J., Der, C. J., Fearon, E. R., Sundaresan, M., Finkel, T., and Goldschmidt-Clermont, P. J. (1997) *Science 275*, 1649−1653.

BI972725U